ChemComm

Accepted Manuscript

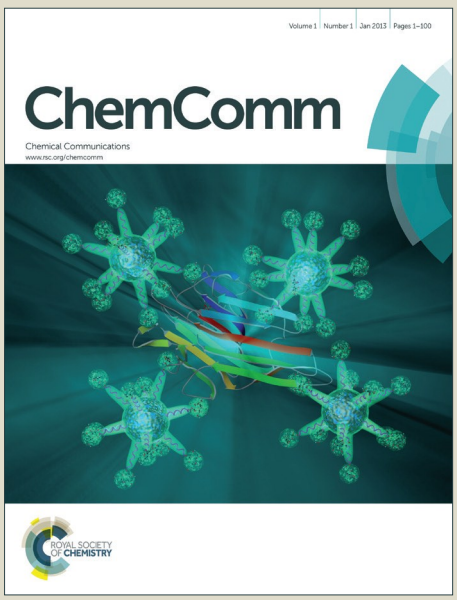

ROYAL SOCIETY OF CHEMISTRY

www.rsc.org/chemcomm

ChemComm

RSCPublishing

COMMUNICATION

Cite this: DOI: 10.1039/x0xx00000x

Tuning the cavities of zirconium-based MIL-140 frameworks to modulate CO_2 adsorption

Received 00th January 2012,
Accepted 00th January 2012

DOI: 10.1039/x0xx00000x

www.rsc.org/

Weibin Liang[a], Ravichandar Babarao[b], Tamara L. Church[a], Deanna M. D'Alessandro[a]*

A combined experimental and computational study has revealed the interplay between the framework pore size and functionality on the CO_2 adsorption performance of zirconium-based MIL-140 frameworks. The CO_2–sorbent interactions were markedly influenced by pore-confinement effects which arise from the π-stacked arrangement of the ligands within the framework backbone.

Rapid increases in the combustion of fossil fuels have led to increasing atmospheric CO_2 concentrations which have been implicated in global warming,[1-4] making the minimisation of anthropogenic emissions from post-combustion flue gas a subject of considerable scientific and technological importance.[1-4] In parallel with the development of renewable energy technologies, the discovery of new materials that capture CO_2 for subsequent sequestration or conversion are urgently required. Compared to conventional solid adsorbents for CO_2 capture such as zeolites, mesoporous silicas and activated carbons, metal-organic frameworks (MOFs) are of particular interest because their surface chemistry and pore architectures can be readily tuned via modular synthesis.[1, 2] By choosing appropriate building blocks, materials having cavities with pre-defined shapes and functionalities can be engineered, providing optimal host/guest interactions.[4-10]

The flue gas from the combustion of coal in air consists of 15–16% CO_2 and 70–75% N_2 (amongst other components including H_2O, SO_x and NO_x), and is released at a total pressure of approximately 1 bar. Thus, CO_2 adsorbents should possess a high CO_2 uptake and selectivity at a partial pressure near 0.15 bar. One strategy towards optimising the ability of MOFs to selectively adsorb CO_2 over other components of a post-combustion flue gas mixture involves engineering the pore environment by introducing functional sites such as coordinatively unsaturated metal centres, amines (alkyl/aryl), azacycles, sulfonic acids, carboxylic acids, sulfones, hydroxyl groups, nitro groups, halogen atoms and/or ionic species.[2, 4, 11-13] While the influence of functional groups on host-guest interactions have been extensively documented, the effect of pore and aperture sizes on CO_2–host interactions are critical issues that are sometimes overlooked in the analysis of such functionalised frameworks.[2]

Recent experimental and computational studies have indicated that a decrease in the pore size within a MOF can augment framework–CO_2 interactions due to the overlap of potential fields between adsorbent surfaces, resulting in a higher affinity and capacity for CO_2.[2, 14-17] For example, post-synthetic exchange of Zr to Ti in the zirconium-based MOF UiO-66 reduces the pore size by ~1 Å leading to significant enhancements in both the CO_2 uptake (2.3 to 4 mmol.g^{-1}) and isosteric heat of adsorption (by ~10 kJ.mol^{-1}).[14]

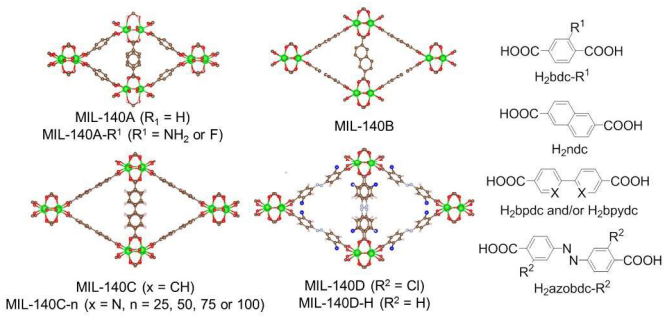

Figure 1. Illustrations of the MIL-140 crystalline structures. The organic linkers that are incorporated into the frameworks are also presented. Colour scheme: Zr, green; C, grey; O, red; N, silver; Cl, blue, H, white.

In the present work, we focus on an emerging class of highly chemically and thermally stable isoreticular MOFs having the MIL-140 topology, which is typified by MIL-140A ([ZrO(bdc)], bdc = 1,4-benzenedicarboxylate), and its analogues including the existing MIL-140A-NH_2, MIL-140A-F, MIL-140B, MIL-140C and MIL-140D solids,[18] in which bdc-NH_2 (2-amino-1,4-benzendicarboxylate), bdc-F (2-fluoro-1,4-benzendicarboxylate), ndc (2,6-naphthalenedicarboxylate), bpdc (biphenyl-4,4'-dicarboxylate), and azobdc-Cl (3,3'-dichloro-4,4'-azobenzenedicarboxylate), respectively, replace the parent bdc ligands of MIL-140A. New members of the series that include bpdc-Me (biphenyl-3,3'-dimethyl-4,4'-dicarboxylate), bpydc (2,2'-bipyridine-5,5'-dicarboxylate), and azobdc (4,4'-azodibenzoate) as linkers are also presented herein (Figure 1).The ability to systematically modulate the pore size and functionality

through ligand engineering[18-20] in MIL-140 has permitted a detailed analysis of the relationship between these parameters and the post-combustion separation abilities of the frameworks, which have been corroborated using Density Functional Theory (DFT) calculations.

In this work, a microwave-assisted solvothermal synthesis protocol previously reported by our group was used to prepare pure phases of high-quality crystalline MIL-140 frameworks (see ESI for full synthesis details).[19, 20] Following their synthesis, the frameworks were washed with *N,N'*-dimethylacetamide (DMA, 3 × 20 mL),[21] methanol (3 × 20 mL), and acetone (3 × 20 mL) and activated at 220 ºC under vacuum (ESI).

Table 1. Comparison of physical properties and CO_2-adsorption performance of MIL-140 MOFs. [22]

Compound	S_{BET} [a] ($m^2.g^{-1}$)	$\alpha_{CO2/N2}$ [b]	$\lvert Q_{st}^0 \rvert$ [c] ($kJ.mol^{-1}$)	$n_{CO2,\ 0.15bar}$ [d] ($mmol.g^{-1}$)
MIL-140A	396.4(0.9)	32.9	30.0	0.16
MIL-140A-NH_2	269.3(0.6)	34.8	34.0	0.28
MIL-140A-F	350.3(0.7)	12.6	36.2	0.10
MIL-140B	429.1(1.1)	18.7	25.1	0.17
MIL-140C	660.8(0.5)	12.9	22.2	0.18
MIL-140C-25	665.9(0.5)	22.2	29.2	0.38
MIL-140C-Me	574.4(1.3)	13.3	20.5	0.21
MIL-140D	830.6(1.9)	8.6	13.3	0.10

[a]Calculated from the N_2 adsorption isotherm measured at 77 K. Values in parentheses indicate the uncertainties; [b]Coadsorption selectivity at 293 K, $\alpha_{CO2/N2} = (Q_{CO2,0.15\ bar}/Q_{N2,\ 0.75\ bar})/(p_{CO2}/p_{N2})$; p = 0.15 bar for CO_2 and 0.75 bar for N_2; [c]Calculated from CO_2 adsorption isotherms measured at 293, 303, and 313 K; [d]Measured at 293 K.

The MIL-140 analogues were first characterised by X-ray powder diffraction (XRPD) to study their crystallinity and stability (ESI). The functionalised materials were isoreticular with their parent structures, as indicated qualitatively by the similarity in their XRPD spectra as well as by *Le Bail* fittings of their cell parameters (ESI): specifically, MIL-140A-NH_2 and MIL-140A-F were isostructural to MIL-140A; MIL-140C-n (n = 25, 50, 75, and 100, molar percentage of bpydc ligands) and MIL-140C-Me were isostructural to MIL-140C; and MIL-140D-H was isostructural to MIL-140D. However, activated MIL-140C-100 and MIL-140D-H constructed solely from bpydc and azobdc linkers, respectively, were unstable in air, and transformed into different phases after four days under ambient conditions (ESI). Attempts to obtain the original crystalline products by resolvating the samples with *N,N*-dimethylformamide (DMF) were unsuccessful (ESI). Further experiments demonstrated that the maximum ratio of bpydc ligands that could be introduced into the MIL-140C structure without inducing this structural transformation was *ca.* 25 molar percent (ESI).[23] Thus, MIL-140A, MIL-140A-R (R = NH_2 and F), MIL-140B, MIL-140C, MIL-140C-25, MIL-140C-Me and MIL-140D were selected for the subsequent experiments.

Thermogravimetric analysis (TGA, see ESI for details) revealed that all frameworks were thermally stable up to *ca.* 450 ºC. The presence of defects within the structures was investigated using TGA under air.[24, 25] MIL-140A, MIL-140A-F, MIL-140B, MIL-140C and MIL-140D were found to be non-defective (ESI); however, MIL-140A-NH_2, MIL-140C-25 and MIL-140C-Me were 8.5, 10.6, and 16.8% lighter, respectively, than expected on the basis of their idealised molecular weights, indicating the existence of missing-linker defects within these frameworks (ESI). A hydrothermal test confirmed that the studied materials are stable in liquid water at room temperature (ESI).

The Brunauer-Emmett-Teller (BET)[26] surface areas and the pore-size distributions (calculated from non-local density functional theory calculations, NLDFT,[27] compared to the N_2 isotherms measured at 77 K) indicated systematic decreases in surface area and pore sizes as a function of the ligand length and cavity functionality (e.g., from 830.6 $m^2.g^{-1}$ and 10.5 Å for MIL-140D to 269.3 $m^2.g^{-1}$ and 5.2 Å for MIL-140A-NH_2; Table 1, Figure 2c and ESI).

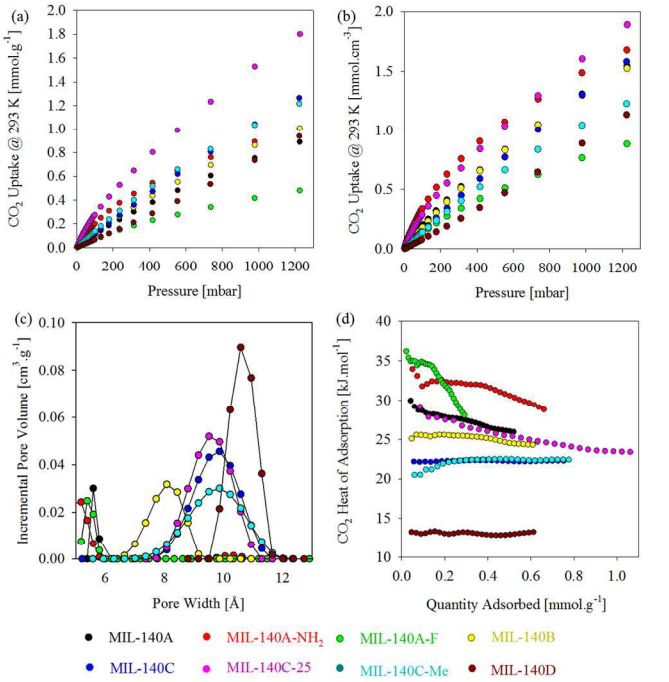

Figure 2. (a) Gravimetric and (b) volumetric CO_2-adsorption isotherms measured at 293 K; (c) Pore size distributions; (d) Isosteric heat of CO_2 adsorption (Q_{st}) for MIL-140 frameworks as a function of the quantity of CO_2 adsorbed.

Due to the industrial emphasis on the volume, rather than the weight of an adsorbent in stationary applications, the volumetric capacity, which takes into account the density and crystallite packing of a material, is often a better indicator of uptake for post-combustion CO_2 capture performance.[28] Figures 2a and b show the gravimetric and volumetric gas adsorption isotherms, respectively, for the MIL-140 series. Compared to literature,[29-32] the gravimetric uptake values for CO_2 reported herein for MIL-140 samples are relatively low due to the small surface areas. MIL-140C-25 showed the highest CO_2 uptake at 1.2 bar and 293 K (1.89 $mmol.cm^{-3}$, Figure 2b, evaluated based upon a crystallographic density of 1.05 $g.cm^{-3}$, see ESI for details), taking up 19.6% more CO_2 per gram than pristine MIL-140C (Figure 2c). A similar finding was recently reported for UiO-67 ($[Zr_6O_4(OH)_4(C_{14}H_8O_4)_6]$),[33] in which the substitution of bpdc ligands with bpydc led to an enhancement in the CO_2 uptake to 8.0 wt% at 1 bar and 293 K.[33] Considering the isostructural relationship between

MIL-140C and MIL-140C-25, and their theoretical pore volumes, the enhanced CO_2 capacity of the latter can be attributed to the incorporation of the Lewis basic bipyridyl sites, and potentially the presence of missing-linker defects. In the present case, at 0.15 bar and 293 K, the CO_2 volumetric capacity decreased in the order MIL-140A-NH_2 > MIL-140C-25 > MIL-140A > MIL-140B > MIL-140C ≈ MIL-140C-Me ≈ MIL-140A-F > MIL-140D (Figure 2b). This trend is consistent with that previously reported in which the introduction of nitrogen-rich functional groups and the reduction in pore size both enhance CO_2 uptake.[10, 11 8, 9, 16, 17, 34]

The CO_2 isosteric heats of adsorption for the MIL-140 MOFs, calculated using the Clausius–Clapeyron equation, are presented in Figure 2d. Pore-confinement effects on the CO_2–sorbent interactions are reflected in the initial enthalpies of adsorption (Q_{st}^0, Table 1). For the parent MIL-140 frameworks, Q_{st}^0 decreased in the order MIL-140A (30.0 kJ.mol^{-1}) > MIL-140B (25.1 kJ.mol^{-1}) > MIL-140C (22.2 kJ.mol^{-1}) > MIL-140D (13.3 kJ.mol^{-1}), which correlates well with the increasing pore sizes of the materials (Table 1 and Figure 2c). In principle, smaller pores will enable more effective potential energy well-overlap between the adsorbent-adsorbate surfaces and will consequently provide a stronger binding environment for CO_2.[14, 35-37] An analysis of the potential correlations between the framework properties and the isosteric heat of adsorption revealed that Q_{st}^0 has a strong relationship ($R^2 > 0.8$) to the pore size, pore volume and BET surface area of the materials (ESI).[38] In addition, Q_{st}^0 values for MIL-140A-NH_2 and MIL-140C-25 are 4 and 7 kJ.mol^{-1} higher than the parent MIL-140A and MIL-140C frameworks, respectively (Table 1).[39] Similar increases in Q_{st}^0 upon functionalisation of a framework with amine or azacycles have been attributed to the effects of acid–base chemistry, electrostatic forces, or enhanced dispersion forces.[1, 8, 9, 11, 34 37]

Surprisingly, MIL-140A-F showed the highest CO_2 affinity in the zero-uptake limit (Q_{st}^0 = 36.2 kJ.mol^{-1}, Table 1). However, a plot of Q_{st} versus the amount of adsorbate per mole (rather than per gram) of absorbent (ESI) showed a sharp decrease in Q_{st} at 0.5 mol.mol^{-1} for MIL-140A-F, which corresponds to ~0.5 CO_2 molecules per bdc-F ligand. This abrupt change in Q_{st} may indicate the presence of two different binding sites within this material. MIL-140 structures are built up from double chains of edge sharing ZrO_7 polyhedra connected through the linear dicarboxylate ligands to define a three dimensional periodic structure with triangular 1-D pores, in which 50 percent of the aromatic linkers are π-stacked. Based on our previous findings,[19] we postulated that π-stacking within the structure modifies the electronic nature of half of the bdc-F ligands in MIL-140A-F, causing stronger CO_2 interactions with these ligands. DFT calculations examining the location and strength of CO_2 binding in MIL-140A-F (ESI) provided strong evidence to support this hypothesis. Thus, in MIL-140A-F, a CO_2 molecule preferentially binds between the fluorine atoms on two adjacent π-stacked ligands. For the 50% of bdc-F ligands that are π-stacked, one CO_2 molecule interacts with both fluorine atoms on two π-stacked ligands and with one hydrogen atom from neighbouring ligands.[40] Thus, Q_{st} for MIL-140A-F decreases sharply as these strong binding sites become saturated (~0.5 mol.mol^{-1}) and CO_2 begins to interact with the weaker binding sites at higher loadings (ESI, Figure S29).

The ideal selectivity for CO_2 over N_2 in flue gas (based on a flue gas composition of 0.15 bar CO_2, 0.75 bar N_2 and 0.1 bar other components) was calculated using two methods: a single-point method using a ratio of uptakes of the two pure component gases at relevant pressures (Table 1), and using Ideal Adsorbed Solution Theory (IAST, ESI).[41] A strong correlation was observed between the framework pore size and the CO_2 adsorption selectivity (ESI). The selectivity factors ($\alpha_{CO2/N2}$) decreased systematically from 32.9 for MIL-140A to 18.7, 12.9, and 8.6 for MIL-140B, MIL-140C, and MIL-140D, respectively (Table 1). This is in contrast to the results of Yaghi and co-workers, who reported that the CO_2 selectivity of eight zeolitic imidazolate frameworks (ZIFs) did not vary with pore diameter, but rather with the functional groups. Such contrasting observations for the ZIF and MIL-140 frameworks may be attributed to the larger pore sizes (7.1–15.6 Å) in ZIFs compared with the MIL-140 series (5.2–10.6 Å).[30] Moreover, in a similar fashion to other MOFs functionalised with basic nitrogen-containing organic groups,[32, 42, 43] grafting MIL-140A and MIL-140C with acrylamine and bipyridyl improved the $\alpha_{CO2/N2}$ value by factors of 1.06 and 1.72, respectively. Additionally, the selectivity factors for CO_2 adsorption over N_2 at 293 K (CO_2/N_2 = 15/85) calculated from IAST (ESI) decreased as a function of framework pore size, reaffirming our observations.

In summary, the synthesis and characterisation of a series of isoreticular Zr-oxo based MIL-140 frameworks, including three new members of the series, has demonstrated the relationship between adsorbent properties, in particular the pore size, and post-combustion CO_2 separation abilities, both experimentally and theoretically. In addition, the structural properties of MIL-140A-F (with regards to the stacked ligands) have provided unique insights into the interaction of CO_2 with the functional groups in the small pores. Our results reveal the crucial function of pore-confinement effects in CO_2–sorbent interactions, which are essential for the design of advanced materials for CO_2 capture.[16, 17, 35-37, 44, 45] Studies to elucidate the function of defects in these MIL-140 solids are ongoing.

This research was supported by the Science and Industry Endowment Fund (SIEF). RB acknowledges the computational facilities and services provided through the CSIRO Scientific Computing, National Computing Infrastructure (NCI) and iVEC@UWA.

Notes and references

[a] School of Chemistry, The University of Sydney, Sydney, New South Wales 2006, Australia.
[b] Manufacturing Flagship CSIRO, Private Bag 33, Clayton South MDC, Victoria 3169, Australia.

Electronic Supplementary Information (ESI) available: Experimental details, XRPD patterns, *Lebail* refinements, TGA curves, ^{1}H NMR spectra and sorption data. See DOI: 10.1039/c000000x/

1. D. M. D'Alessandro, B. Smit and J. R. Long, *Angew. Chem., Int. Ed.*, 2010, **49**, 6058-6082.
2. Y.-S. Bae and R. Q. Snurr, *Angew. Chem., Int. Ed.*, 2011, **50**, 11586-11596.
3. K. Sumida, D. L. Rogow, J. A. Mason, T. M. McDonald, E. D. Bloch, Z. R. Herm, T.-H. Bae and J. R. Long, *Chem. Rev.*, 2012, **112**, 724-781.

4. Z. Zhang, Z.-Z. Yao, S. Xiang and B. Chen, *Energy Environ. Sci.*, 2014, **7**, 2868-2899.
5. W. Lu, Z. Wei, Z.-Y. Gu, T.-F. Liu, J. Park, J. Park, J. Tian, M. Zhang, Q. Zhang, T. Gentle Iii, M. Bosch and H.-C. Zhou, *Chem. Soc. Rev.*, 2014, **43**, 5561-5593.
6. H. Furukawa, K. E. Cordova, M. O'Keeffe and O. M. Yaghi, *Science*, 2013, **341**, 974.
7. T. Devic and C. Serre, *Chem. Soc. Rev.*, 2014, **43**, 6097-6115.
8. Q. Yang, A. D. Wiersum, P. L. Llewellyn, V. Guillerm, C. Serre and G. Maurin, *Chem. Commun.*, 2011, **47**, 9603-9605.
9. G. E. Cmarik, M. Kim, S. M. Cohen and K. S. Walton, *Langmuir*, 2012, **28**, 15606-15613.
10. Y.-S. Bae, O. K. Farha, J. T. Hupp and R. Q. Snurr, *J. Mater. Chem.*, 2009, **19**, 2131-2134.
11. A. Das and D. M. D'Alessandro, *CrystEngComm*, 2015, **17**, 706-718.
12. S. Biswas, J. Zhang, Z. Li, Y. Y. Liu, M. Grzywa, L. Sun, D. Volkmer and P. Van Der Voort, *Dalton Trans.*, 2013, **42**, 4730-4737.
13. A. Das, P. D. Southon, M. Zhao, C. J. Kepert, A. T. Harris and D. M. D'Alessandro, *Dalton Trans.*, 2012, **41**, 11739-11744.
14. C. Hon Lau, R. Babarao and M. R. Hill, *Chem. Commun.*, 2013, **49**, 3634-3636.
15. Y. Huang, W. Qin, Z. Li and Y. Li, *Dalton Trans.*, 2012, **41**, 9283-9285.
16. J. An and N. L. Rosi, *J. Am. Chem. Soc.*, 2010, **132**, 5578-5579.
17. Y.-X. Tan, Y.-P. He and J. Zhang, *Chem. Commun.*, 2011, **47**, 10647-10649.
18. V. Guillerm, F. Ragon, M. Dan-Hardi, T. Devic, M. Vishnuvarthan, B. Campo, A. Vimont, G. Clet, Q. Yang, G. Maurin, G. Ferey, A. Vittadini, S. Gross and C. Serre, *Angew. Chem., Int. Ed.*, 2012, **51**, 9188.
19. W. Liang, R. Babarao and D. M. D'Alessandro, *Inorg. Chem.*, 2013, **52**, 12878-12880.
20. W. Liang and D. M. D'Alessandro, *Chem. Commun.*, 2013, **49**, 3706-3708.
21. Due to the higher solubility of dicarboxylate ligands in DMA than DMF, DMA was selected for use in the activation procedure.
22. See ESI for a full table of properties for MIL-140 frameworks.
23. ^{1}H NMR analysis was applied to confirm the actual bpydc ligand loading in the MIL-140C-25 samples (see ESI for detail).
24. G. C. Shearer, S. Chavan, J. Ethiraj, J. G. Vitillo, S. Svelle, U. Olsbye, C. Lamberti, S. Bordiga and K. P. Lillerud, *Chem. Mater.*, 2014, **26**, 4068-4071.
25. S. Chavan, J. G. Vitillo, D. Gianolio, O. Zavorotynska, B. Civalleri, S. Jakobsen, M. H. Nilsen, L. Valenzano, C. Lamberti, K. P. Lillerud and S. Bordiga, *Phys. Chem. Chem. Phys.*, 2012, **14**, 1614-1626.
26. S. Brunauer, P. H. Emmett and E. Teller, *J. Am. Chem. Soc.*, 1938, **60**, 309-319.
27. Based on the N_2-Cylindrical Pores – Oxide Surface DFT model in the MicroActive software package, Micromeritics Instruments Inc.
28. A. Das, M. Choucair, P. D. Southon, J. A. Mason, M. Zhao, C. J. Kepert, A. T. Harris and D. M. D'Alessandro, *Microporous Mesoporous Mater.*, 2013, **174**, 74-80.
29. R. Banerjee, A. Phan, B. Wang, C. Knobler, H. Furukawa, M. O'Keeffe and O. M. Yaghi, *Science*, 2008, **319**, 939-943.
30. R. Banerjee, H. Furukawa, D. Britt, C. Knobler, M. O'Keeffe and O. M. Yaghi, *J. Am. Chem. Soc.*, 2009, **131**, 3875-3877.
31. X. Si, C. Jiao, F. Li, J. Zhang, S. Wang, S. Liu, Z. Li, L. Sun, F. Xu, Z. Gabelica and C. Schick, *Energy Environ. Sci.*, 2011, **4**, 4522-4527.
32. E. Stavitski, E. A. Pidko, S. Couck, T. Remy, E. J. M. Hensen, B. M. Weckhuysen, J. Denayer, J. Gascon and F. Kapteijn, *Langmuir*, 2011, **27**, 3970-3976.
33. L. Li, S. Tang, C. Wang, X. Lv, M. Jiang, H. Wu and X. Zhao, *Chem. Commun.*, 2014, **50**, 2304-2307.
34. S. Couck, J. F. M. Denayer, G. V. Baron, T. Remy, J. Gascon and F. Kapteijn, *J. Am. Chem. Soc.*, 2009, **131**, 6326-6327.
35. P. Deria, J. E. Mondloch, E. Tylianakis, P. Ghosh, W. Bury, R. Q. Snurr, J. T. Hupp and O. K. Farha, *J. Am. Chem. Soc.*, 2013, **135**, 16801-16804.
36. P. Nugent, Y. Belmabkhout, S. D. Burd, A. J. Cairns, R. Luebke, K. Forrest, T. Pham, S. Ma, B. Space, L. Wojtas, M. Eddaoudi and M. J. Zaworotko, *Nature*, 2013, **495**, 80-84.
37. S. D. Burd, S. Ma, J. A. Perman, B. J. Sikora, R. Q. Snurr, P. K. Thallapally, J. Tian, L. Wojtas and M. J. Zaworotko, *J. Am. Chem. Soc.*, 2012, **134**, 3663-3666.
38. We assume that the small pore size in the MIL-140 structure leads to monolayer adsorption for CO_2, which is similar to the concept of BET surface area (single-layer adsorption of N_2 on the surface).
39. DFT calculations show that the initial binding site for CO_2 in MIL-140A-NH_2 is the amine group in the structure.
40. Distances between the carbon atom in the CO_2 molecule and two seperate fluorine atoms on two different π-stacking bdc-F ligands are 3.10 and 3.17 Å; distances between one oxygen atom in the CO_2 molecule and two hydrogen atoms on two π-stacking bdc-F ligands are 2.78 and 2.71 Å.
41. A. L. Myers and J. M. Prausnitz, *AIChE J.*, 1965, **11**, 121-127.
42. J. An, S. J. Geib and N. L. Rosi, *J. Am. Chem. Soc.*, 2010, **132**, 38-39.
43. H. Yin, J. Wang, Z. Xie, J. Yang, J. Bai, J. Lu, Y. Zhang, D. Yin and J. Y. S. Lin, *Chem. Commun.*, 2014, **50**, 3699-3701.
44. D.-X. Xue, A. J. Cairns, Y. Belmabkhout, L. Wojtas, Y. Liu, M. H. Alkordi and M. Eddaoudi, *J. Am. Chem. Soc.*, 2013, **135**, 7660-7667.
45. J.-R. Li, J. Yu, W. Lu, L.-B. Sun, J. Sculley, P. B. Balbuena and H.-C. Zhou, *Nat. Commun.*, 2013, **4**, ncomms2552, 2558 pp.

